Retrieval of Cloud Phase Using the Moderate Resolution Imaging Spectroradiometer Data during the Mixed-Phase Arctic Cloud Experiment

D. Spangenberg
Analytical Services and Materials, Inc.
Hampton, Virginia

P. Minnis
NASA-Langley Research Center
Hampton, Virginia

M. Shupe and T. Uttal
NOAA Environmental Technology Laboratory
Boulder, Colorado

M. Poellot
University of North Dakota
Grand Forks, North Dakota

Introduction

Improving climate model predictions over Earth's polar regions requires a comprehensive knowledge of polar cloud microphysics. Over the Arctic, there is minimal contrast between the clouds and background snow surface, making it difficult to detect clouds and retrieve their phase from space. Snow and ice cover, temperature inversions, and the predominance of mixed-phase clouds make it even more difficult to determine cloud phase. Also, since determining cloud phase is the first step toward analyzing cloud optical depth, particle size, and water content, it is vital that the phase be correct in order to obtain accurate microphysical and bulk properties. Changes in these cloud properties will, in turn, affect the Arctic climate since clouds are expected to play a critical role in the sea ice albedo feeback (Curry et al. 1996). The previous work of Minnis et al. (1995) provides a liquid and ice phase detection scheme but it does not use enough channels to separate mixed phase, ice, and liquid clouds. However, because of their predominance in the Arctic, mixed phase clouds need to be considered in a satellite cloud property retrieval algorithm. Strabala et al. (1994) and Baum et al. (2000) used a trispectral infrared (IR; 8.5-12 μm) algorithm to determine cloud phase over non-polar regions. In this application, the brightness temperature difference (BTD) between 8.5 and 11 μm (T85-11) and the BTD between 11 and 12 μm (T11-12) are plotted on a scatter diagram used to determine cloud phase. Although the trispectral IR technique works reasonably well to discriminate ice phase from liquid and mixed phase clouds, it, like the method of Minnis et al. (1995), fails to discriminate liquid from mixed phase clouds. This is the case since mixed-phase Arctic clouds tend have liquid drops at their tops (Rangno and Hobbs 2001) and frequently appear as liquid clouds in the trispectral infrared (IR)

technique. In this study, the mixed phase cloud is defined to be one that has either stratified layers of liquid and ice or liquid and ice co-existing in the same volume of space in the cloud.

Since the Moderate Resolution Imaging Spectroradiometer (MODIS) has three water vapor (WV; 6.7-8.5 μm) channels, each measuring radiation from a different tropospheric level, they can be used to detect different types of polar cloud systems. Previous studies have used National Oceanic and Atmospheric Administration (NOAA) High-Resolution Infrared Sounder/2 (HIRS/2) and MODIS data in the WV region of the spectrum to aid in detection of clouds in polar regions (Ackerman 1996; Liu et al. 2004). In this paper, the IR trispectral technique (IRTST) is used as a starting point for a WV and 11-μm brightness temperature (T11) parameterization (WVT11P) of cloud phase using MODIS data. In addition to its ability to detect mixed-phase clouds, the WVT11P also has the capability to identify thin cirrus clouds overlying mixed or liquid phase clouds (multiphase ice). Results from the Atmospheric Radiation Measurement (ARM) MODIS phase model (AMPHM) are compared to the surface-based cloud phase retrievals over the ARM North Slope of Alaska (NSA) Barrow site and to in-situ data taken from University of North Dakota Citation (CIT) aircraft which flew during the Mixed-Phase Arctic Cloud Experiment (MPACE). It will be shown that the IRTST and WVT11P combined to form the AMPHM can achieve a relative high accuracy of phase discrimination compared to the surface-based retrievals. Since it only uses MODIS WV and IR channels, the AMPHM is robust in the sense that it can be applied to daytime, twilight, and nighttime scenes with no discontinuities in the output phase.

Data

Terra and *Aqua* MODIS 1-km 6.7 (T67), 7.3 (T73), 8.5 (T85), 11 (T11), and 12 (T12) μm brightness temperature data are averaged onto a 10-km radius circular region centered at the ARM-NSA Barrow site. These brightness temperature data are used as input to the MODIS phase model. The surface-based cloud phase retrievals used to validate the AMPHM consist of 1-minute and 90-meter resolution time-height cross-sections. The details of the surface-based phase retrieval scheme can be found in Shupe et al. (2005). Additionally, surface-retrieved liquid water path (LWP) data is derived from the microwave radiometer based in Barrow and the ice water path (IWP) is determined using the millimeter-wave cloud radar regression technique (Shupe et al. 2001, 2005). These water paths are required to estimate the ratio of liquid water to ice in mixed-phase clouds. For Citation in-situ data, the liquid water content and total water content, which are used to compute the relative percentage of liquid water in mixed phase clouds, were obtained from the King and CSI probes, respectively. Atmospheric profile data used in this study were recorded by ARM radiosondes launched from NSA-Barrow. National Weather Service radiosonde data was used for times when the ARM data was either missing or incomplete.

Moderate Resolution Imaging Spectroradiometer Cloud Phase Model

The WVT11P works on the premise that different cloud types will usually be associated with distinct patterns in the thermal and moisture profiles inside and above the cloud. Since the difference in brightness temperature between the MODIS water vapor channels is coupled to the thermal and moisture structure of the atmosphere, it will be indirectly linked to the cloud type and hence cloud phase. For a

standard sub-Arctic winter atmosphere free of clouds, Liu et al. (2004) showed that the MODIS 6.7-µm weighting function (WF) peaks near 600mb (or 4 km) and the 7.3-µm WF peaks near 800mb (or 2 km). The 8.5-µm WF will have a peak near the surface with a shape identical to the 11-µm WF.

A set of four distinct clouds types was found while developing the AMPHM. These include boundary layer liquid, low-mid level mixed, high ice, and low ice. Ice clouds with tops above 3 km are considered to be of the high ice variety. Figure 1 shows the cloud top height distribution for each cloud phase. Liquid clouds tend to be found at or below 1 km and mixed-phase clouds have a peak just below 1 km with a broad tail toward higher cloud tops. For ice-phase clouds, the distribution is bi-modal with a large peak for cloud tops near and above 6 km and a secondary peak between 0.5 and 1.0 km. The corresponding mean temperature (T) and dewpoint (Td) profiles for the ice and mixed-phase cases are shown in Figure 2a. Each cloud type has its own distinctive profile. The liquid and mixed profiles in Figure 2b also show a distinct difference with the liquid phase clouds exhibiting a stronger T inversion with dry air above the tops of the shallow clouds.

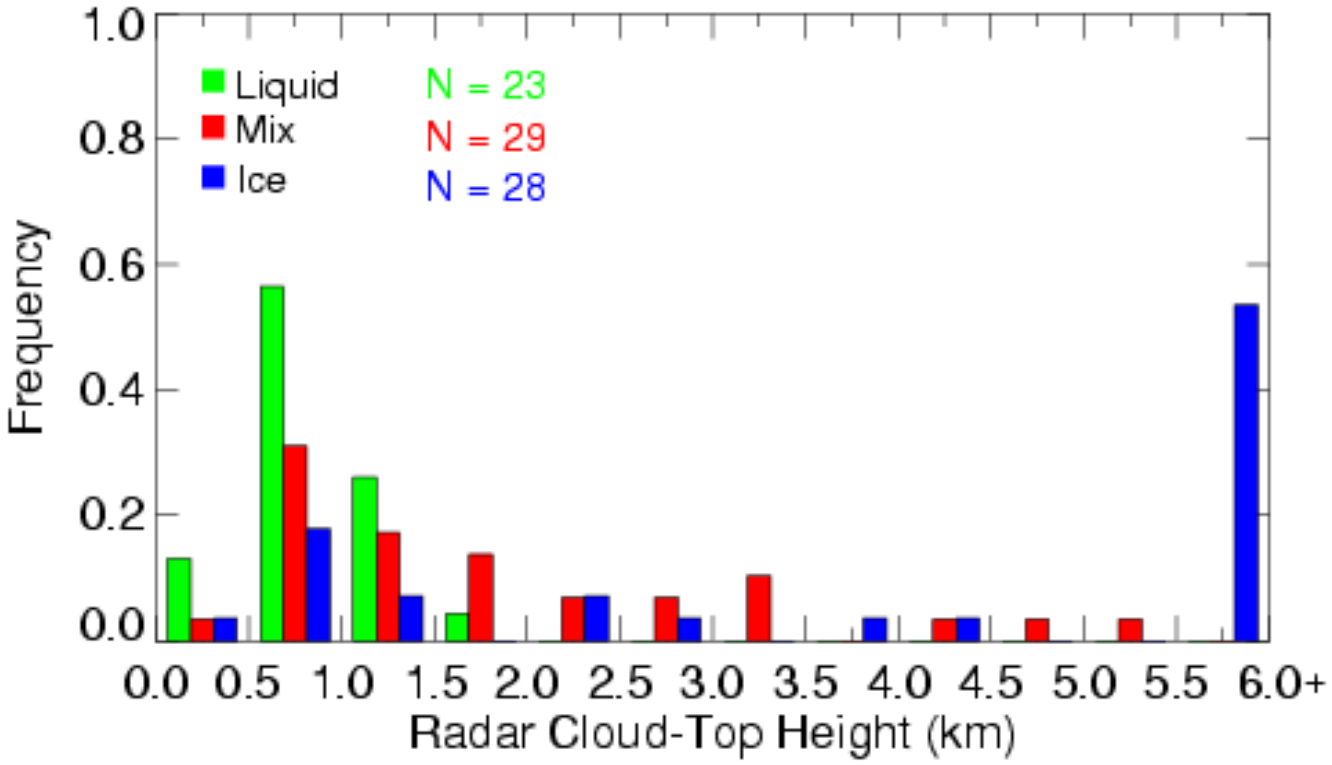

Figure 1. Cloud height distribution for the selected cases used to develop the MODIS cloud phase model.

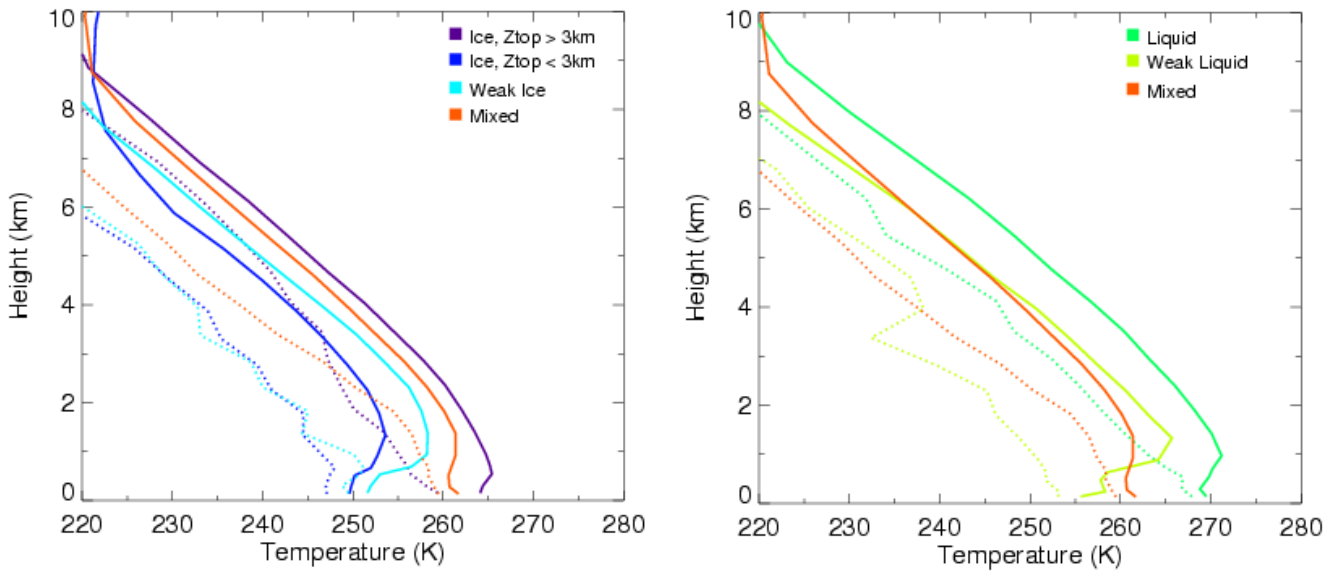

2a 2b

Figure 2. Mean sounding profiles for the selected phase model cases. Mixed and ice profiles are shown in (a) while (b) shows mixed and liquid profiles. Solid lines are for temperature and dotted lines are for dewpoint temperature. Ztop represents the cloud-top height. The weak ice category is for those ice clouds found in the boundary layer only.

The beginning point for the MODIS phase model for polar clouds is the IRTST. Ice and liquid have similar absorption coefficient values at 8.5 μm, however, at 11 μm, the absorption coefficient of ice is larger than for water (Strabala et al. 1994). This causes ice clouds to exhibit a positive T85-11 since the radiation at T11 will be arriving at the satellite from a higher, colder layer in the cloud. Contrary to the larger T11-12 values for water clouds found in the standard IRTST, the opposite tends to be true for polar clouds because of the frequent T inversions and cold surface. Yamanouchi et al. (1987) found that the T11-12 values in thin clouds tend to be higher when the cloud top temperature is lower than the background surface and negative if the cloud top is warmer than the surface. This leads to separation in T11-12 between cirrus clouds and boundary layer liquid and mixed-phase clouds trapped in the frequent temperature inversions. Figure 3a shows the T85-11 and T11-12 scatter diagram for 96 cases from the years 2000-2004 used to develop the AMPHM. The color-coding indicates the surface-retrieved cloud phase. The selected cases represent a wide range of meteorological conditions so that most, if not all, cloud types were sampled. Clouds with T85-11 values over 0.35 K are considered to have an ice phase. The other regions on Figure 3a are those where mixed-phase clouds are typically found and consequently where the WVT11P is required. Note the greatest concentration of mixed-phase clouds are found roughly halfway between the ice and liquid cases.

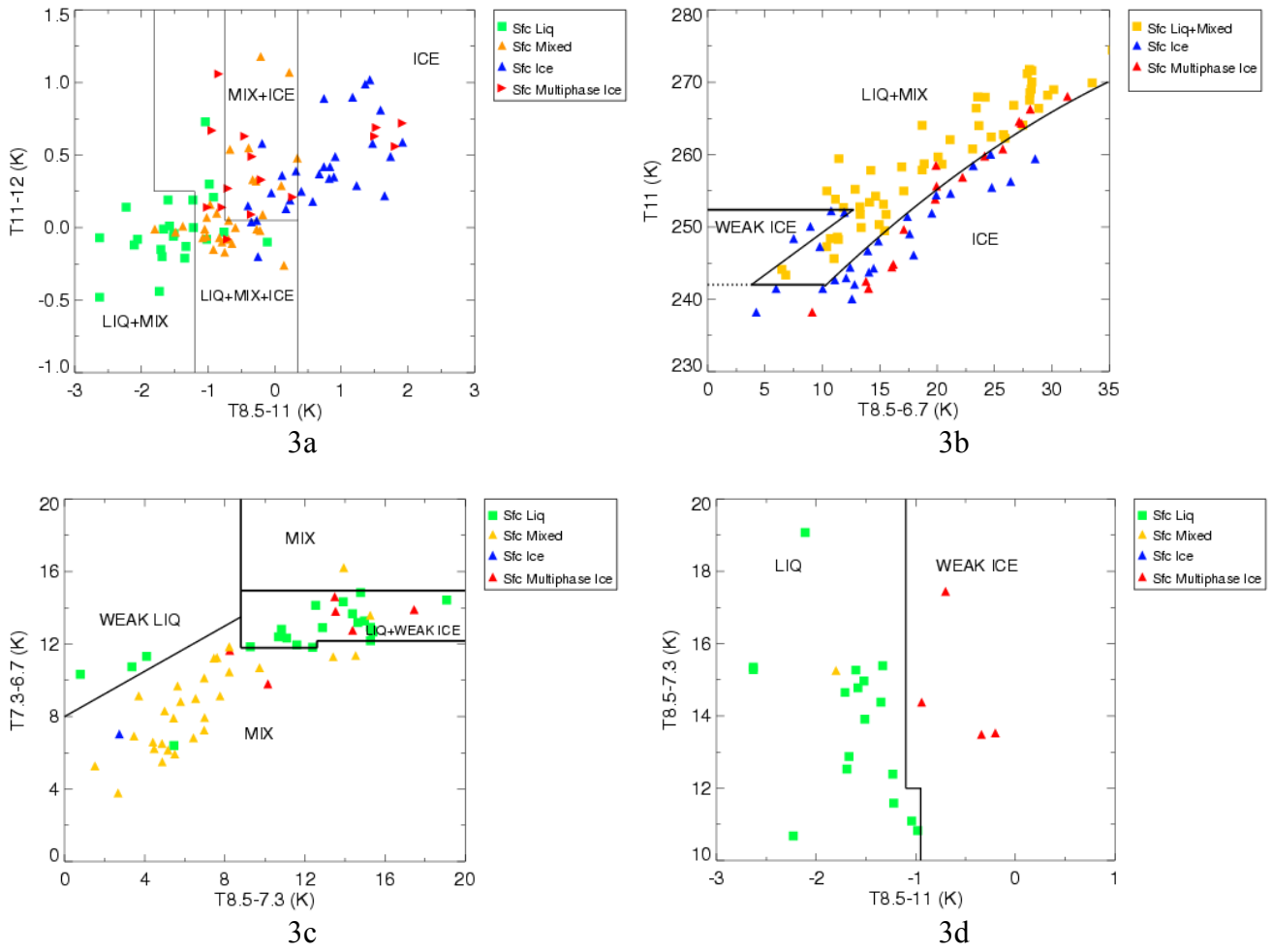

Figure 3. MODIS cloud phase model development. Diagram (a) is used to group pixels into the initial phase categories using T85-11 and T11-12. Diagram (b) shows T85-67 plotted against T11; it is used to separate ice from the mix and liquid phases. Diagram (c) shows T85-73 plotted against T73-67; it is used to distinguish the mixed phase from liquid and multiphase ice. Diagram (d) shows T85-11 plotted with T85-73; it is used to separate the liquid phase from multiphase ice. Points are plotted in color to represent the surface (sfc) phase retrieval.

For the mixed-phase and ice overlap region of Figure 3a (top-center), and across the center of the diagram where all three phases are found, the T85, T67 BTD (T85-67) and T11 part of the WVT11P is applied to separate out the ice phase from the mixed and liquid clouds. This part of the parameterization is shown in Figure 3b; it includes each of the AMPHM cases from Figure 3a. The blue and red points are for the surface-retrieved ice and multiphase ice, respectively, while orange points represent liquid and mixed phase. Any MODIS pixel falling below the solid black line will be assigned the ice phase, which is in agreement with the surface phase retrievals. Most ice-phase clouds lie in the lower-right part of the diagram with high T85-67 values. This occurs because there is a relatively large amount of water vapor above high ice clouds so that the radiation sensed by MODIS at 6.7 μm will be from a layer mostly above cloud top with the T85 radiation coming from inside the cloud. The T and Td profiles for high ice clouds shown in Figure 2a indicate that on average, the upper layers are nearly saturated to the tropopause. Moreover, examination of the relative humidity (RH) at cloud top and the mean RH from

cloud top to 1 km above the top (not shown) revealed no significant drop in RH. For the mixed and liquid region in Figure 3b (above the black solid line), dry air exists above cloud top and the T85-67 is driven primarily by the difference in temperature between the middle troposphere and cloud top. The area in the lower-left part of Figure 3b is a special subset of thin, boundary-layer ice crystal clouds that do not show up well in any of the MODIS satellite images and some of these cases could be diamond dust. These cases have small T85-67 values since the 6.7-μm WF drops down to the lower troposphere during the cold, dry Arctic winter, peaking at a level not far above the 8.5-μm WF. Many of the multiphase ice cases, where thin cirrus overlies a mixed or liquid cloud, will be put into the ice phase. For those multiphase ice cases falling in the liquid and mixed region, it is likely that some of the pixels within 10 km of Barrow will actually be grouped into the ice phase since thin cirrus tends to be organized into streamers and filaments.

To assign a cloud phase to MODIS pixels in the liquid and mixed overlap region of Figure 3a (lower-left), and for the center of the diagram where all three phases are found, the T85, T73 BTD (T85-73) and T73, T67 BTD (T73-67) part of the WVT11P is used to separate out the mixed phase from the liquid phase. This stage of the parameterization is depicted in Fig. 3c; it includes each of the cases above the black solid line in Figure 3b. Since mixed-phase clouds are found in a wide variety of T, WV conditions in the Arctic, a larger part of the diagram must be devoted to them. The mixed-phase clouds on the right-hand side of Figure 3c are relatively warm with cloud top temperatures generally ranging from 260 to 270 K. These are the most difficult types of mixed-phase clouds to separate from the liquid phase. Warm-season liquid-phase clouds in the boundary layer by themselves only occur in a specific set of meteorological conditions and this is reflected by the tight cluster of liquid phase cases in the upper-right part of Figure 3c. The liquid phase cases in the upper-left part of the diagram represent cold-season cases where large temperature inversions are found with the cloud trapped in the cold boundary-layer air. Only one surface-retrieved liquid cloud phase case lies in the mixed-phase part of the diagram. This is a case where the microwave radiometer LWP is relatively low with a weaker T inversion compared to the liquid cases on the upper-left part of the Figure 3c diagram and it could be a mixed-phase cloud. Conversely, just one surface-retrieved mixed-phase cloud lies in the liquid part of the Figure 3c diagram. This is a rare case where the synoptic conditions mimic the liquid-phase clouds. The WVT11P cannot separate this and so it will become a liquid-phase cloud in the AMPHM. One final step is taken to discriminate the liquid phase from multiphase ice clouds. For the cases in the liquid and weak ice region of Figure 3c, their T85-11 and T85-73 values are plotted together in Figure 3d, revealing that the weak, or multiphase, ice points can be separated from the liquid ones largely by their T85-11 values with the stronger-absorbing ice having higher T85-11 values.

The order of each test in the AMPHM developed for polar clouds is critical to the outcome and it is summarized in Figure 4. First, any pixel with a T11 over 273 K is assigned the liquid phase. The next step is to screen the low T11 pixels below 242 K as ice clouds. The IRTST is then applied and the resulting pixels are either grouped into the ice phase or passed on to the WVT11P. Pixels falling in the mixed and ice phase region of Figure 3a will next have their T85-67 and T11 values checked and will be grouped into the ice or mixed phase accordingly. MODIS pixels falling in the mixed and liquid region of Figure 3a will be tested by the T85-73, T73-67 part of the WVT11P to screen for mixed-phase clouds. For any MODIS pixel in the center of the Figure 3a diagram in the liquid, mixed, and ice overlap region, the T85-67, T11 test is first applied (Figure 3b). If the pixel isn't classified as ice, the T85-73, T73-67 test is run (Figure 3c) to separate out the mixed phase. Since multiphase ice pixels are likely to be found

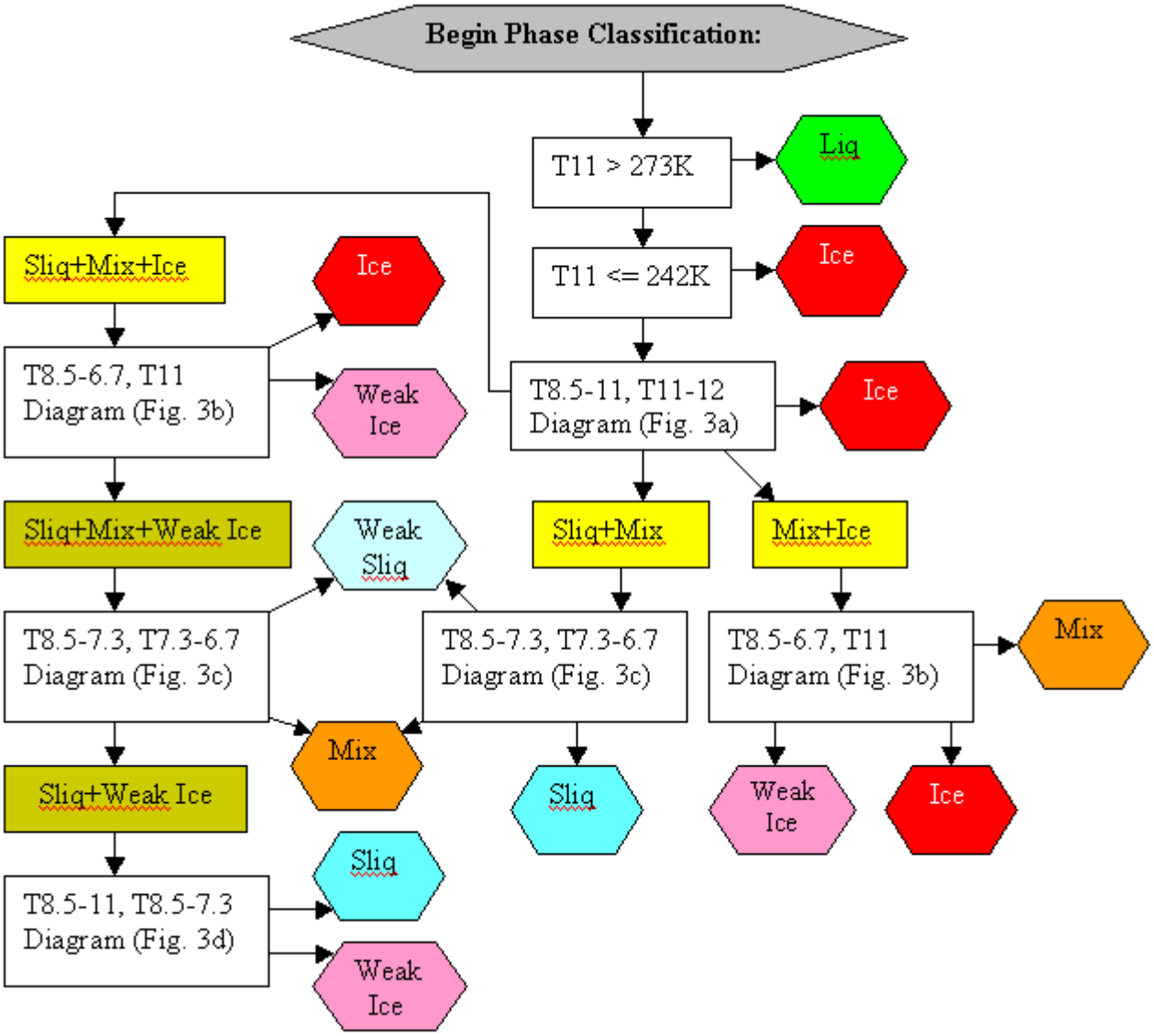

Figure 4. AMPHM schematic. White boxes are for the T, BTD tests, yellow boxes are for the different phase groupings in the IRTST, and light green boxes are where the phase could not be finalized from a given test and subsequent test(s) are initiated. Colored hexagons are ending points for the determined phase. Liq is for liquid water and Sliq represents supecooled liquid water.

in the center of the IRTST diagram (Figure 3a), any pixel falling into the liquid and weak ice overlap region of Figure 3c will have its T85-11 and T85-73 values checked (Figure 3d) to separate out the multiphase ice.

Results

To assess the performance of the AMPHM, the surface-based phase retrievals of Shupe et al. (2005) were compared to the AMPHM-retrieved phase for 92 Terra and Aqua orbits during MPACE. For the

validation procedure, the AMPHM output represents the dominant phase signal from pixel-level image data averaged over 10-km-radius circular region centered at Barrow. In order to be used in the validation dataset, a single phase must be present in the surface-based phase retrieval across the cloud top for, at least, 1 hour before and after the satellite overpass. The validation results are summarized in Table 1. Most of the cases were mixed phase with an agreement slightly better than 80% between the surface and satellite phase retrievals. The ice agreement is somewhat better, near 86%, with the 7 liquid cases at 100% agreement. It should be pointed out that the AMPHM was developed for a wide variety of atmospheric conditions not all of which were found during MPACE. Additionally, the validation includes overlapping, multiple phase clouds systems, the surface retrievals do not break down thin cloud layers into more than one phase, and Barrow is on the coast where land and sea differences will complicate the comparisons. Taking these factors into account, the AMPHM validation results during MPACE are remarkably good.

Table 1. MODIS and surface-retrieved matched phase data during MPACE.

Phase	Matching%	N
Mixed	80.4	56
Ice	86.2	29
Liquid	100.0	7

Once the phase is determined, it is important to know the relative amounts of liquid and ice in the mixed phase clouds. To determine how mixed the mixed phase clouds were during MPACE, the LWP from the microwave radiometer was compared to the IWP retrieval from the surface-based sensors at the ARM-NSA Barrow site. Results of this comparison are shown in Figure 5. The relative amount of liquid compared to ice in the clouds is almost exclusively between 10 and 90%, with a large cluster of values ranging from 60-80%. For those cases where the AMPHM incorrectly retrieved the liquid phase, the relative amounts of liquid in the cloud were high, with values over 60%. Conversely, when the AMPHM retrieved ice instead of the mixed phase, the relative liquid amounts were low, at or below 40%. Also plotted in Figure 5 are 10-minute average data samples from the CIT when it was within 20 km of Barrow. The black triangles are for those times when the plane was at least 0.5 km or more below cloud top and the red triangles represent times when it was within 0.5 km of cloud top. There is far more liquid in the clouds near the top compared to the amount deep inside the cloud, confirming the theory on mixed-phase clouds. Moreover, there is good agreement between the CIT in-situ data, the AMPHM retrievals, and surface-based retrievals.

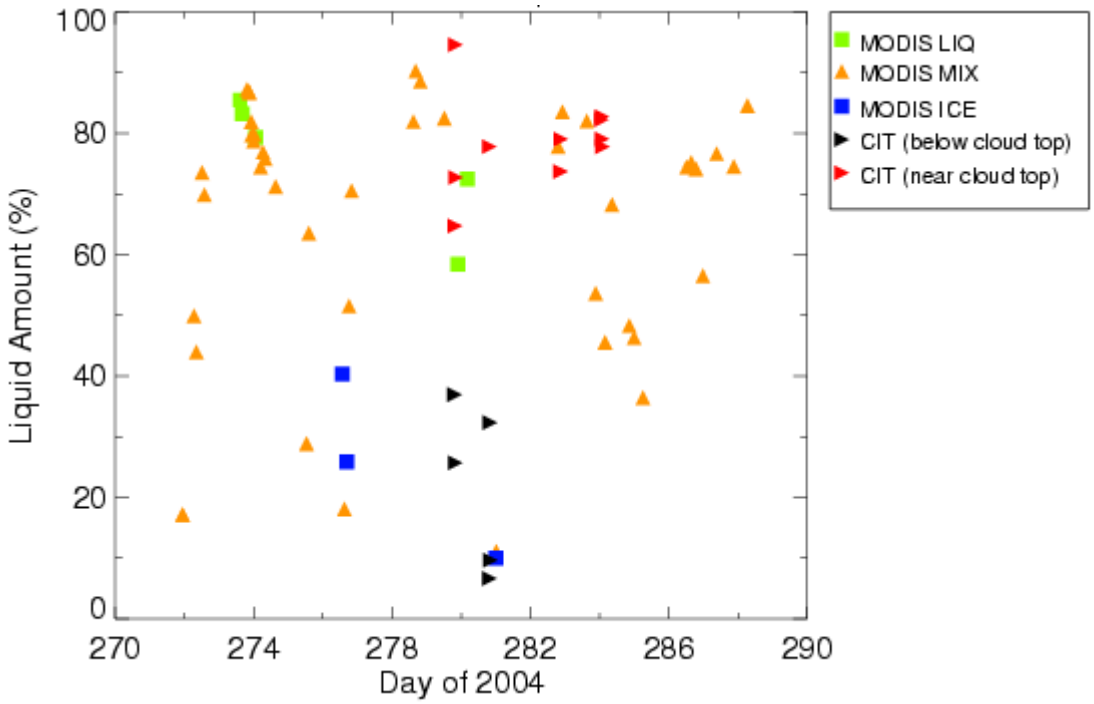

Figure 5. The surface-derived relative liquid amount in mixed-phase clouds for Terra and Aqua overpass times during MPACE. Symbols are color-coded to show the MODIS cloud phase type. Also shown are the CIT relative liquid amounts for times when the aircraft was within 20 km of the ARM-NSA Barrow site.

For mixed–phase clouds, the T85-11 values found during MPACE were compared to T85-11 values in the multi-year dataset used to develop the AMPHM. It is interesting to note that these BTD values are significantly lower during MPACE with a mean near –1.60 K whereas the multi-year dataset has a mean value closer to –0.80 K. This suggests that most of the mixed-phase clouds sampled during MPACE had an unusually large amount of liquid across their tops compared to the amount of ice. This reasoning will hold for temperatures increasing downward from the cloud top, which occurs when the cloud top is either at the inversion base or above the inversion peak. This placement of the cloud with respect to the inversion was found to hold for most of the mixed-phase clouds used in developing the AMPHM.

To show the spatial extent of the AMPHM results, the Clouds and the Earth's Radiant Energy System (CERES) cloud mask of Trepte et al. (2002) was first applied to the Terra MODIS imagery taken at 2115 UTC, 9 October 2004. This is a case when the CIT was transiting from Deadhorse to Barrow during MPACE. Before using the AMPHM, the T67 image was filtered using a 2-dimensional fast-Fourier transform technique to remove noise from the image's power spectra. The resulting cloud phase image from the AMPHM is shown along with the corresponding satellite imagery in Figure 6. The T11 image in Figure 6a shows a uniform stratus cloud with values ranging from 255-265 K. The T85-11 image in Figure 6b shows that a relatively large amount of liquid exists near cloud top over the far western part of the domain. These pixels have T11 values that are quite variable, ranging from 250-265 K. The corresponding T85-11 values are near –2.0 K. A small portion of this area becomes supercooled liquid at the periphery of the mixed-phase cloud at higher T11 and higher T85-73 values (see Figures 6a, c, and d). The area in the northwestern part of the domain has relatively low T11 values

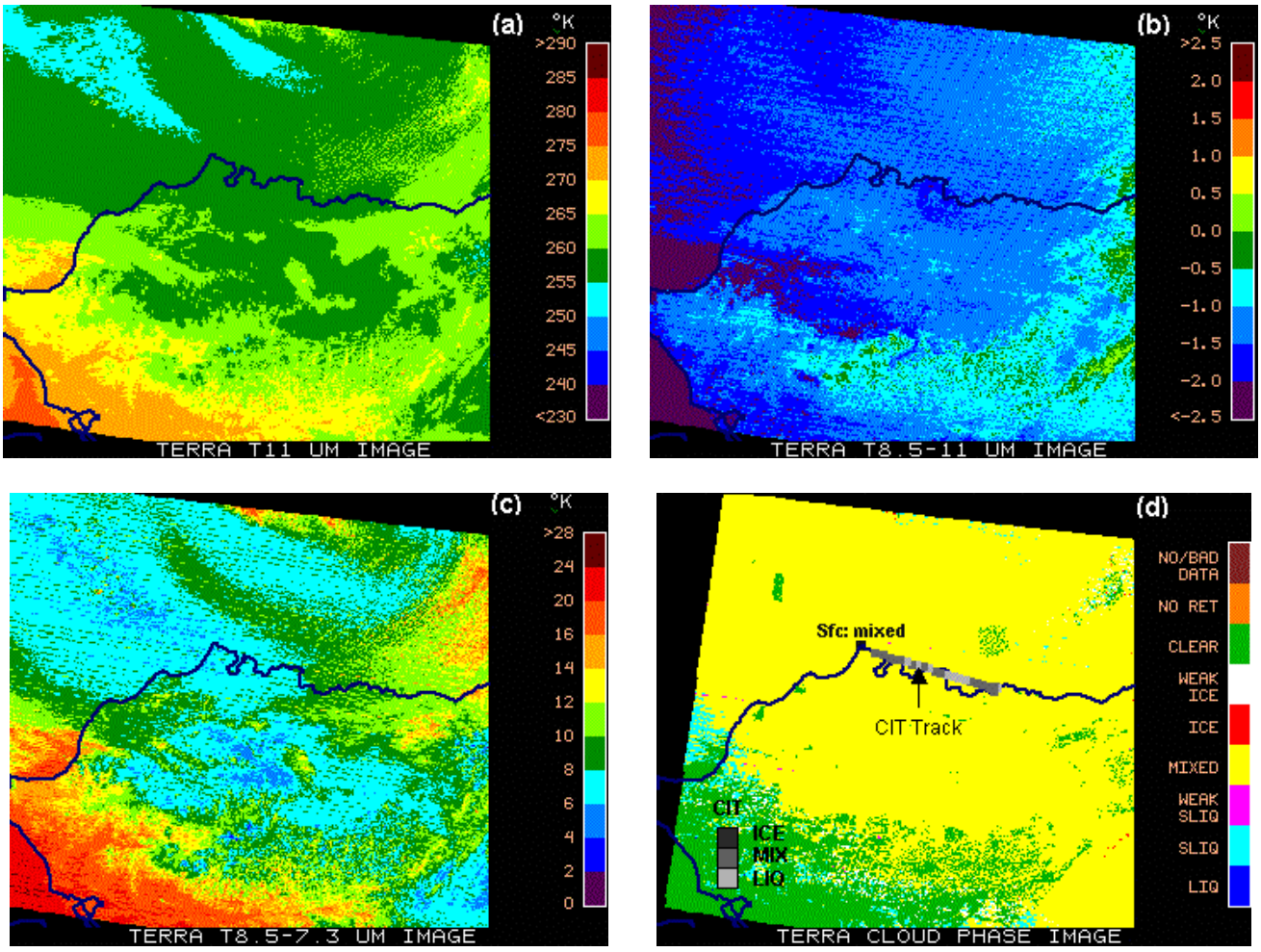

Figure 6. *Terra*-MODIS imagery for 21:15 UTC, 9 October 2004. (a) The 11 μm image is shown in (a), (b) is the 8.5-11 μm image, (c) is the 8.5-7.3 μm image, and (d) is the MODIS phase model image. Also plotted on (d) are the surface-based phase retrieval and the CIT flight track. Gray shades indicate the phase sampled by the CIT. The liq and sliq terms in the phase colorbar in (d) represent liquid water and supercooled liquid water, respectively.

and low T85-73 values. These are mixed phase clouds with points lying on the left side of the WV parameterization in Figure 3c. The phase over most of this extensive stratus cloud is retrieved as mixed in the AMPHM, a result that cannot be explained by the water and ice absorption coefficient theory implicit in the T85-11 image of Figure 6b. The surface phase retrieval at Barrow also shows the phase to be mixed. For the CIT transit, the phase was determined by averaging the liquid water content and total water content in 2-minute time intervals. Relative liquid amounts from 10-90 % are considered to be mixed phase. Figure 6d shows the CIT flight path, plotted in gray shades to indicate the phase. Mostly a mixed phase cloud was sampled with some liquid phase, probably at cloud top. This is in agreement with the AMPHM and surface-based phase retrievals.

Conclusions

In this study, a MODIS cloud phase detection model was developed for polar cloud systems. This model starts with an IR trispectral technique utilizing the difference in the absorption coefficient of ice and liquid water between the 8.5 and 11 μm MODIS channels along with the BTD between 11 and 12 μm. Since mixed-phase clouds typically appear to be either all ice or all liquid water in this scheme, a water vapor and 11-μm brightness-temperature parameterization was developed to separate the mixed-phase pixels from those containing exclusively ice or liquid water. Using the parameterization will allow for the detection of mixed phase clouds even when only liquid water is found at their tops. A set of 92 cases examined during the Mixed-Phase Arctic Cloud Experiment revealed that the MODIS cloud phase model has a classification accuracy of 80-100% compared to the surface-based phase retrievals at Barrow. For the mixed-phase clouds sampled during MPACE, the LWP and IWP from the surface-based retrievals and the CIT in-situ data confirmed that they generally had between 10 and 90% liquid water relative to the amount of ice. However, using the MODIS T85-11 test revealed that the many of the mixed-phase clouds during MPACE had unusually large amounts of water relative to ice at their tops. The AMPHM also showed an ability to correctly identify the ice phase for multiphase ice clouds. Of the 16 model cases of thin cirrus existing with clouds having other phases below them, 14 were correctly identified as being ice crystals and the remaining 2 were classified as mixed phase. The main strengths of the MODIS phase classification technique is that it will work just as well in cloud shadows, nighttime, and twilight scenes as it does for fully sunlit conditions. However, it is unclear how it will perform over highly elevated terrain such as the Antarctic plateau. Also, near phase transitions, the model may have some difficulties due to abnormally moist or dry layers that can sometimes exist above the cloud top.

Once cloud phase is determined, the next step is to use the methods of Minnis et al. (2003) and Platnick et al. (2001) to determine the cloud microphysical properties. The current algorithms are set up to detect and process the ice and liquid phase only and presently cannot be tuned to retrieve polar cloud properties. Since mixed-phase clouds tend to have liquid at their tops, a realistic droplet size can likely be retrieved, with a modification based on the assumed amount of liquid water content at the top of the cloud taken from T85-11. Also, the current algorithms produce ice crystal diameters that are either too small or non-existent for mixed-phase clouds due to water droplet contamination. It may be possible to develop a parameterization of the ice crystal diameter in mixed-phase clouds in terms of cloud temperature, optical depth, water droplet size, and atmospheric thermal and water vapor structure.

Corresponding Author

Douglas Spangenberg, d.a.spangenberg@larc.nasa.gov, (757) 827-4647

Acknowledgements

This research was supported by the Environmental Sciences Division of U.S. Department of Energy Interagency Agreement DE-AI02-97ER62341 under the ARM program. Data were obtained from the ARM Program sponsored by the U.S. Department of Energy, Office of Science, Office of Biological and Environmental Research, Environmental Sciences Division.

References

Ackerman, SA. 1996. "Global satellite observations of negative brightness temperature differences between 11 and 6.7 μm." *Journal of the Atmospheric Sciences*, 53(19)2803-2812.

Baum, BA, PF Soulen, KI Strabala, MD King, SAAckerman, WP Menzel, and P Yang. 2000. "Remote sensing of cloud properties using MODIS airborne simulator imagery during SUCCESS, 2, Cloud thermodynamic phase." *Journal of Geophysical Research* 105(D09)11,781-11,792.

Curry, JA, WB Rossow, D Randall, and JL Schramm. 1996. "Overview of Arctic cloud and radiation characteristics." *Journal of Climate* 9:1731-1764.

Liu, Y, JR Key, RA Frey, SA Ackerman, and WP Menzel. 2004. "Nighttime polar cloud detection with MODIS." *Remote Sensing of Environment* 92:181-194.

Minnis, P., et al., 1995: Cloud Optical Property Retrieval (Subsystem 4.3). In Clouds and the Earth's Radiant Energy System (CERES) Algorithm Theoretical Basis Document, Vol. III: Cloud Analyses and Radiance Inversions (Subsystem 4), NASA RP 1376 Vol. 3, edited by CERES Science Team, pp. 135-176.

Minnis, P, DF Young, S Sun-Mack, PW Heck, DR Doelling, and QZ Trepte. 2003. "CERES cloud property retrievals from imagers on TRMM, Terra, and Aqua. SPIE Tenth International Symposium, Remote Sensing." *Conference on Remote Sensing Clouds and Atmosphere*, Barcelona, Spain, September 8-12, 37-48.

Platnick, SJ, Y Li, MD King, H Gerber, and PV Hobbs. 2001. "A solar reflectance method for retrieving cloud optical thickness and droplet size over snow and ice surfaces." *Journal of Geophysical Research* 106(D14)15,185-15,199.

Rangno, AL and PV Hobbs. 2001. "Ice particles in stratiform clouds in the Arctic and possible mechanisms for the production of high ice concentrations." *Journal of Geophysical Research* 106(D14)15,065-15,075

Shupe, MD, T Uttal, SY Matrosov, and AS Frisch. 2001. "Cloud water contents and hydrometeor sizes during the FIRE Arctic Clouds Experiment." *Journal of Geophysical Research* 106(D14)15,015-15,028.

Shupe, MD, T Uttal, and SY Matrosov. 2005. "Arctic cloud microphysical retrievals from surface-based remote sensors at SHEBA." *Journal of Applied Meteorology*. In press.

Strabala, KI, SA Ackerman, and WP Menzel. 1994. "Cloud properties inferred from 8-12-μm data." *Journal of Applied Meteorology* 33, 212-229.

Trepte, QZ, P Minnis, and RF Arduini. 2002. "Daytime and nighttime polar cloud and snow identification using MODIS data." In *Proceeding of the SPIE Conference on Optical Remote Sensing of the Atmosphere and Clouds III*, Hangzhou, China, October 23-27.

Yamanouchi, T, K Suzuki, and S Kawaguchi. 1987. "Detection of clouds in Antarctica from infrared multispectal data of AVHRR." *Journal of the Meteorological Society of Japan* 65(06) 949-961.